ICSE6-212

An ex-situ scour testing device for characterizing erosion of cohesive soils

Haoyin Shan[1], Kornel Kerenyi[2], Junke Guo[3], J. Jerry Shen[4], Andreas Wagner[4] and Zhaoding Xie[4]

[1]Research Engineer, Turner-Fairbank Highway Research Center
GENEX Systems, 6300 Georgetown Pike, McLean, VA 22101
haoyin.shan.ctr@dot.gov

[2]Associate Professor, Dept. of Civil Engineering,
Univ. of Nebraska-Lincoln, PKI 204D, Omaha, NE 68182
jguo2@unl.edu

[3]Hydraulic Research Program Manager, FHWA Hydraulic R&D Program
Department of Transportation, 6300 Georgetown Pike McLean, VA 22101
kornel.kerenyi@dot.gov

[4]Research Engineer, Turner-Fairbank Highway Research Center
GENEX Systems, 6300 Georgetown Pike, McLean, VA 22101
jerry.shen.ctr@dot.gov, andreas.wagner.ctr@dot.gov, and zhaoding.xie.ctr@dot.gov

Abstract*: Erosion in cohesive soils is challenging. It requires a better understanding of forces acting on soil clumps since cohesive soils entrain in a form of clumps. Unfortunately, such information is rarely available due to the slow development of sensors that are capable to capture these forces. An innovative direct force gauge (DFG) in an ex-situ scour testing device (ESTD) was developed to study forces acting on cohesive soil specimens, and to analyze the incipient erosion process. Similar to Couette flow, the ESTD uses a moving belt and a pump to propel the flow in a channel underneath the belt. The channel is 58 cm long, 12 cm wide and 2 cm deep. This well-controlled physical model mimics the near-bed flow of open channel reproducing hydrodynamic forces on cohesive bed soils. Specimens are mounted on a sensor disk that is servo controlled. The reaction forces of the servo controlled DFG equals to erosion forces acting on soil specimens. The pump and two cascaded filter cylinders enable clear flow conditions near soil specimens. When both belt and pump are operating a log-low velocity profile in the near boundary layer can be achieved. The erosion of artificial Kaolin clay specimens reveals the shear stress deceases with the erosion, while the vertical force is hard to predict because it depends on both weight loss of the specimen and the attenuation of the lift force. The mass loss after intermittent running can calculate the erosion rate of soil specimens. Two types of Kaolin are tested in the ESTD and the hole erosion test in the French Institute of Sciences and Technology for Transport, Development and Networks (IFSTTAR). Discrepancy between the critical shear stress exists and possible reasons are discussed.*

Keywords: Erosion, cohesive soils, Couette flow, direct force gauge

I INTRODUCTION

Cohesive soils include silt and clay. With a diameter less than 2 μm, the particle usually has a shape of small flat plates, needles or tubes with a high specific area defined as the ratio of surface area to volume (Partheniades 2009). These particles are subjected to physicochemical forces that are larger in comparison to their weight. Unlike non-cohesive sediments, which resist scouring mostly by their submerged weight, cohesive soils resist scouring by physicochemical forces. The effect of the submerged particle weight is usually negligible (Raudkivi and Tan 1984).

Understanding the physicochemical forces on the micro level is quite challenging, and may not be practical since the scour of cohesive soils is in a form of clumps instead of single particle. Researchers developed several devices to study the scour in cohesive soils by measuring the forces in the scour process. Moore and Masch (1961) developed a circular Couette flow erosion device (CCFED). The device consists of a stationary circular soil specimen mounted on a support that is attached to a torsion wire. An outer drum, concentric with the soil specimen, contains the eroding fluid between it and the soil specimen. The outer drum is rotated by a variable speed motor and a shear stress is consequently transmitted to the soil specimen surface, which can be directly measured by knowing the angular displacement of the torsion wire. Erosion rate of cohesive sediments can be evaluated by knowing the mass difference of the specimen within a time interval.

[1] Corresponding author

Besides the CCFED, other apparatus were proposed with calculated critical shear stress studying the erosion in cohesive soils. These devices include the erosion function apparatus (EFA, Briaud et al. 2001), hole erosion test (HET, Wan and Fell 2004), jet erosion test (JET, Hanson 1991), sediment erosion rate flume (SERF, Sheppard and Bloomquist 2005), sediment erosion at depth flume (SEDflume, McNiel et al. 1996) and adjustable shear stress erosion and transport flume (ASSET, Robert et al. 2003). Trammell (2004) detailed the motivation, testing procedures, data analysis, advantages and limitations of the ASSET, EFA, SEDflume and SERF. The followings focus on the description of HET and JET.

In a HET test, a pinhole is bored in the center of a clay specimen that is inserted into a confining tube connected by two water tanks with different water levels. Water flows through the hole, exerts shear stress to erode the specimen. The flow velocity is increased steadily until entrainment happens. At the end of each increment, the eroded outflow is collected to obtain the erosion rate, and calculate the average diameter of the enlarged hole. The shear stress is caculated from the head loss. The friction coefficient can be obtained from the Moody chart. An erosion curve can be drawn between the erosion rate and the shear stress. Usually, it comes with a function as (Wan and Fell 2004):

$$\dot{\varepsilon} = C(\tau - \tau_c) \tag{1}$$

where $\dot{\varepsilon}$ = the erosion rate; C = the slope of the erosion curve; τ = hydraulic shear stress along the hole; and τ_c = critical shear stress for the initiation of erosion.

In a JET test, an adjustable constant-head tank supplies water to an impinging jet in a tube submerged in an open tank which covers a sediment surface. By converting potential energy to kinetic energy, the jet obtains a certain velocity to erode the sediments. Common jet nozzle has a diameter of 6.4 mm. The nozzle height above the soil surface can be adjusted in a range of 40 to 220 mm. One point gage having an equivalent diameter of the nozzle can go through the jet tube and nozzle, shut off the jet and measure the erosion depth. Thus, the erosion rate has a dimension of height per time. The instant shear stress is calculated by (Hanson and Cook 2004):

$$\tau_i = \tau_0 \left(\frac{J_p}{J_i}\right)^2 \tag{2}$$

where τ_i = instant peak boundary shear stress; τ_0 = maximum shear stress due to the jet velocity at the nozzle, calculated as $\tau_0 = 0.00416\rho(2gh)$, and h = nozzle height above the soil surface; J_p = potential jet core length, equals 6.3 times of the jet nozzle diameter; J_i = instant jet orifice height. For a jet having a 6.4-mm-diameter nozzle, the instant shear stress can be determined as $\tau_i = 0.13h / J_i^2$. The critical shear stress is determined based on the equilibrium scour depth, J_e. Since the equilibrium scour depth requires a long time to reach, it is extrapolated from measured scour depth data by fitting them with a hyperbolic function. By replacing J_i with J_e in Eq. (2), one can calculate the critical shear stress, τ_c.

Among the aforementioned seven devices, ASSET flume, EFA, SEDflume and SERF simulate the duct flow erosion. HET simulates seepage process, and JET simulates erosion under a jet. The CCFED simulates a shallow circular Couette flow erosion process. For bridge design purpose, a device can simulate the erosion process in the open channel flow is extremely needed. Meanwhile, correct prediction of the erosion in cohesive soils requires a better understanding of forces acting on cohesive soils in the erosion process. Unfortunately, such information is rarely available due to the slow development of sensors capable to capture these forces. In this paper, the authors proposed a new ex-situ device which can greatly mimic the near-bed flow of open channels to erode cohesive soils. It also equips with a servo-controlled direct force gauge measures instantaneously hydrodynamic forces on the specimens accommodated on top of its sensor disk.

II EX-SITU SCOUR TESTING DEVICE

Figure 1 shows the concept and 3-D drawings of the ESTD. Its inlet and outlet tanks are connected with a well-defined inner channel in the middle tank by trumpets. The two trumpets smoothly guide the flow. The total volume of 550 liters ensures the fluid near clay specimens is always clear enough for observation.

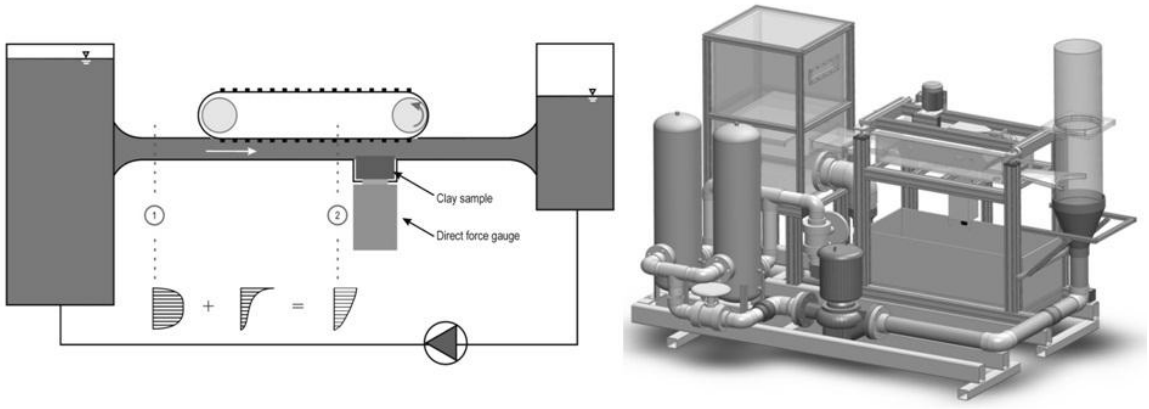

Figure 1: The ex-situ scour testing device (ESTD).

The flow is propelled by a moving belt mounted above the inner channel and a centrifugal pump. The pump was original designed to compensate the energy loss caused by two cascaded filter cylinders that help to clear the fluid in the system. The extra power from the pump generates a higher water level in the inlet tank that produces a conduit flow in the inner channel. In combination with the Couette flow generated by the belt, it reproduces a log-law profile as in the open channel flow (Shan et al. 2011).

The ESTD is capable to instantaneously measure horizontal shear force and vertical force by an innovative direct force gauge. Tested clay specimen sits on top of the gauge. The measured forces are exactly those acting on soil specimens. This makes it capable of capturing varying forces when the shape of soil specimens changes due to erosion. The sensor chamber can accommodate a cylindrical soil specimen with a diameter of 63.5 mm and a maximum height of 15 mm. The sensor disk is positioned on a platform, which can be continuously pushed up/down to any desired position.

III FLOW VELOCITY SUPERPOSITION

Shan (2010) described in detail the PIV system used at the hydraulics laboratory in the Turner Fairbank Highway Research Center (TFHRC). The laser emitter was placed beside the ESTD. Emitted laser beam was converted into a sheet through a laser optic. After reaching a mirror underneath the ESTD tank, the sheet was reflected upward to illuminate a plane in the flow. The flow was seeded with silver-coated hollow glass spheres which have a median diameter of 16 μm, and a density of 1300 kg/m^3. With 20% weight of silver coated on the surface, the spheres can brightly reflect the laser light and generate brilliant spots on PIV images. The image size was 10 mm by 10 mm. The flow can be adjusted by controlling both the pump and the belt. The control parameter can be either pump power/belt speed or energy grade/belt speed. The PIV tests were originally conducted by configuring the pump power and belt speed. Later, the flow conditions were switched to energy grade/belt speed control. Energy grade was measured from the different water levels in the head tank and tail tank at a certain belt speed. The pump power was automatically adjusted to obtain the desired water level.

The flow velocity profile driven only by the moving belt is S-shape (Shan 2010). PIV measurements revealed the pump and the belt together produced a velocity profile significantly agrees with that of an open channel flow. Figure 2 demonstrated this superposition. The circular dots, in a curve similar to a parabola, form the velocity profile when only the pump runs at a frequency of 13 Hz. The square dots create the profile when only the belt runs at a speed of 3.0 m/s. The triangle dots compose the velocity profile when both the pump and the belt run at above conditions. The black line in comparison against triangle dots is a typical log-law velocity profile proposed by Guo (2007). As can be seen, the superposed velocity profile has about 60% (12 mm) of the flow depth that agrees with the log-law profile. Detailed observation leads to that: the influence of the belt is negligible at the bottom since the profile at this part is considerably close to that of only pump runs. While beyond this point, the belt's influence to the profile dramatically increased. Evidently, the profile still has a tail of S-shape curve on the top.

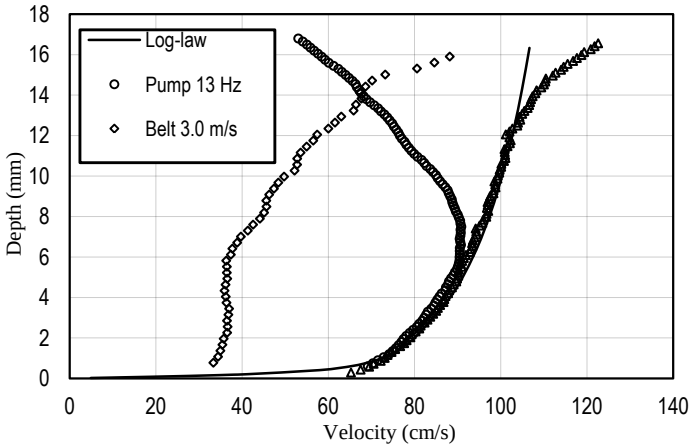

Figure 2: Velocity superposition to a log-law profile in the ESTD.

IV EROSION OF ARTIFICIAL COHESIVE SOIL SPECIMENS

At current stage, only artificial porcelain clay specimens were tested in the ESTD. The preparation procedure of these specimens, their erosion, the measurement of forces acting on them in the erosion, and preliminary analysis were followed.

IV.1 Specimen preparation and erosion

Artificial EPK Kaolin and Armoricaine Kaolin specimens were prepared in the laboratory. Both materials have the same chemical composition: 45% SiO_3 and 37% Al_2O_3. They have a same optimum water content of 26%. However, the EPK Kaolin is finer-graded than Armoricaine Kaolin. The former has a specific surface area of 22 m^2/g, while the later is 9 m^2/g. The EPK Kaolin has a D_{50} of 1 μm, while D_{50} of Armoricaine Kaolin is 2.5 μm (Chevalier and Haghighi 2011).

Since the water content of field clay is unavailable, several arbitrary water contents (31.7% to 52.5%) were assumed. Desired amounts of dry Kaolin powder and distilled water were mixed in a standard 6-inch-diameter proctor for 1 minute. The mixture was quickly transferred into a 63.5-mm-diameter consolidation ring. One saturated filter paper and one porous stone were placed on each end to drain the specimen during the 3-hour compaction with a pressure of 62 KPa. Then the specimen was extracted and trimmed to the desired height with a wire saw. The specimen was fixed onto an aluminum tray, and kept in a closed zip bag for 2 hours before mounted onto the sensor disk.

When mounting, the soil surface was carefully adjusted to be flush with the ESTD tank bottom by elevating or lowering the sensor disk. Then the whole system is filled up to a certain water level. After venting all the air in the system, one can start the flow by setting a desired water level in the inlet tank and a certain belt speed.

In the erosion process, we intermittently stopped the ESTD after certain periods (e.g. 3 minutes). The soil specimen surface will change due to the erosion, and it might need to be elevated in order to keep the flush condition. Since the erosion is not always uniform over the specimen surface, it was challenging to determine the amount of elevation. The erosion then started again, and the above procedure was repeated until the test finished. The whole erosion process was recorded to synchronize with the measured data for post-processing.

IV.2 Analysis of EPK Kaolin test

Figure 3 gives a typical set of instantaneously measured shear stress and normal stress of a EPK Kaolin specimen. The flow had an average velocity of 1.0 m/s. The clay has a water content (mass) of 48%. Its wet and dry bulk densities are 1660 and 1120 kg/m^3. The porosity and degree of saturation are 57.7% and 93.8%, respectively. Figure 3 indicates the critical shear stress for this specimen was less than 10 Pa. The flow stops 4 times during the test, and each running was about 90 seconds. As can be clearly seen, the measured shear stress near the 2nd intermission around 175 seconds did not change too much comparing against other intermissions. This was because the soil specimen was not elevated after the 2nd intermission, while followed other intermissions was an elevation. The elevation amounts can also be compared by the immediate increase of the shear stress, e.g., the 4th elevation was less than other intermissions. The 3rd elevation was the highest.

During each run, the shear stress generally kept decreasing while at several spots it went up and then fell like the fluctuation around 55 seconds. The video recording tells what happened at that moment. A bulk clump was

dislodged from the soil specimen, but it did not leave the soil. Almost half of it crossed the gap, like a bridge across the soil specimen and the sensor chamber. But its lower end still touched the soil specimen. Due to the protrusion of the clump, the form drag dramatically increased. This doubled the measured shear stress from 9 to 18 Pa. Meanwhile, this protrusion blocked the flow at the upstream end of the clump, and generated downward flow which increased the normal force. This clump was washed away around 60 seconds. Then the shear stress dropped back around 10 Pa, and the normal stress resumed around 65 Pa.

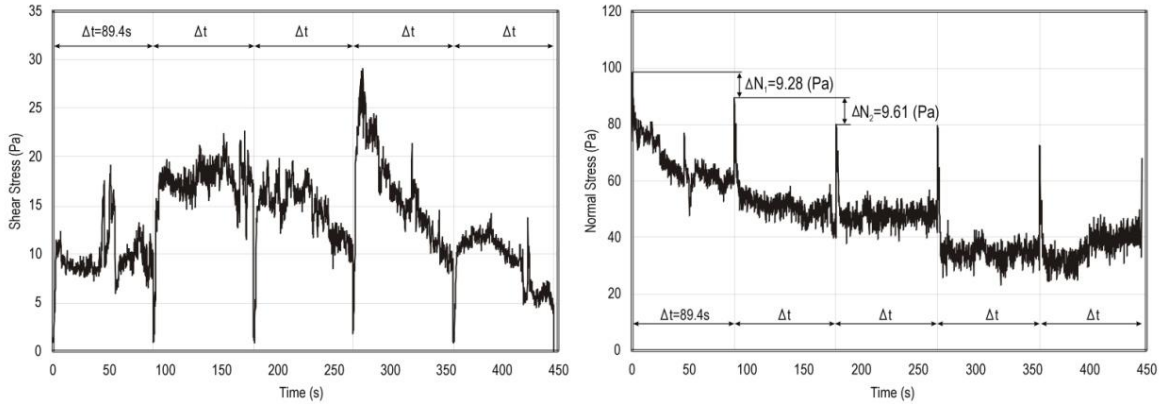

Figure 3: The shear and normal stress recorded in one EPK Kaolin erosion test.

The vertical forces measured by the force gauge include the submerged weight of the soil specimen and the lift force acting on it. In the erosion process, the submerged weight decreased because of material loss. The material loss generated concave shape on surface of the soil specimen, which reduced the lift force. Combining these two decays together, it is difficult to predict the trend of normal force. In the first three running periods, the vertical forces decreased, while it increased in the last two running periods.

IV.3 Analysis of Armoricaine Kaolin test

An Armoricaine Kaolin specimen with a water content of 40.2% was prepared. Its wet and dry bulk densities are 1720 and 1230 kg/m3. Figure 4 shows 5 intermissions existed in the erosion test. The average velocity was 0.8 m/s.

In Figure 4, the left ordinate represents the shear stress, and the right ordinate symbols the soil position. As can be seen, the shear stress during the erosion process kept descending. After elevating the specimen, the gradient of shear stress changed. However, it was not conclusive whether or not the gradient is a function of the elevating amount. The critical shear stress to describe the entrainment point of the erosion was less than 10 Pa.

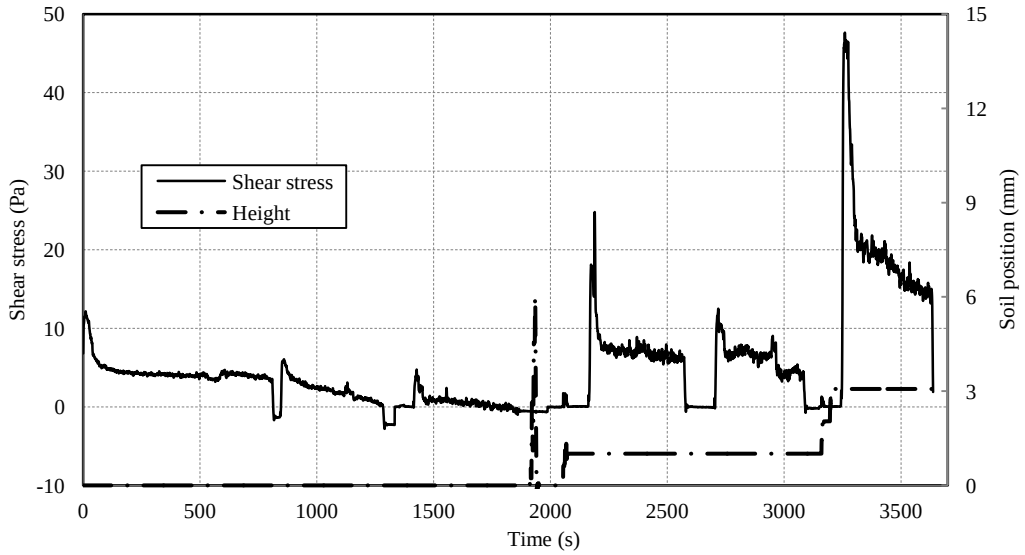

Figure 4: The shear stress recorded in one Armoricaine Kaolin erosion test.

In Figure 5, the left ordinate represents the normal stress and the remaining mass of the specimen in the erosion process. The right ordinate symbols the soil position. The same conclusion can be drawn as tests of

EPK Kaolin that the normal stress in the process is difficult to predict due to the descending soil weight and instantaneously varying lift.

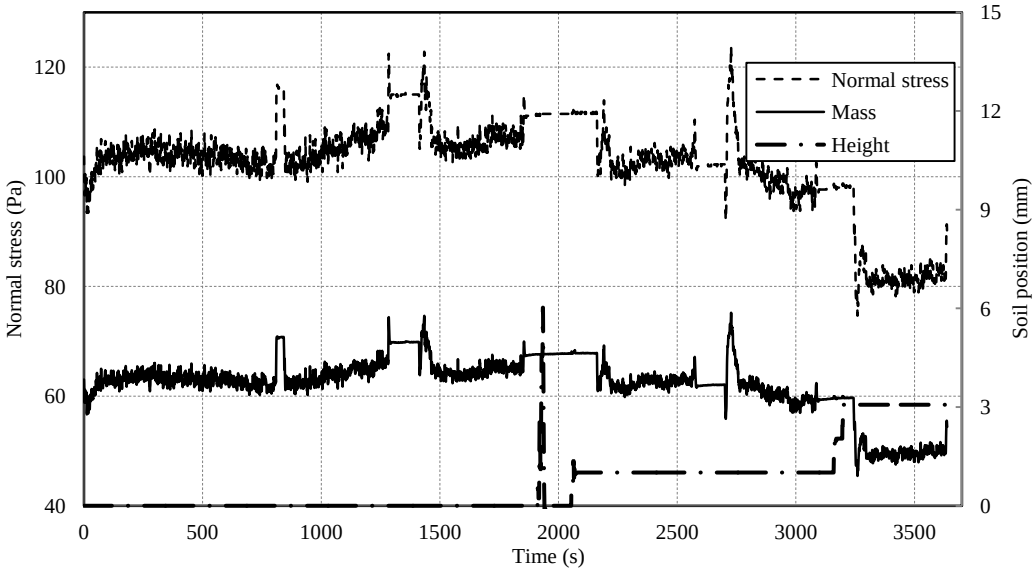

Figure 5: The normal stress recorded in one Armoricaine Kaolin erosion test.

Comparison results between EPK Kaolin and Armoricaine Kaolin in the ESTD reveal they have similar erosion phenomenon when prepared in same procedure and eroded in the ESTD. The critical shear stress of both Kaolin materials is less than 10 Pa.

Chevalier and Haghighi (2011) prepared the EPK Kaolin specimen using standard proctor compaction method. Their HET tests showed the critical shear stress of EPK Kaolin is nearly 1200 Pa. Difference of two orders magnitude exists. This can be explained by the calculation of shear stress in both devices. The ESTD directly measures the shear force, while the HET computes it from the head loss through the whole sample. The head loss includes the inlet loss, the outlet loss and shear loss over the sample surface. Inlet and outlet of samples in the HET has a funnel shape after the erosion instead of a pinhole. This is the adjustment of flow, and indicates the inlet and outlet loss must be excluded in the shear stress calculation. Meanwhile, the different erosion mechanism should also account for the discrepancy.

V CONCLUSIONS

The current ESTD produces fine-tuned near-bed velocity profile, the direct measurement of biaxial stress (shear/normal) on soil specimens. By superposing the conduit flow generated by the pump and the Couette flow by the moving belt, a log-law profile is achieved up to 60% of the flow depth above the ESTD tank bottom. By mounting the specimens right on the sensor disk of the force gauge, the horizontal shear and vertical forces can be neatly acquired. These are exact forces acting on soil specimens unlike the separated sensor and soil specimens in previous studies.

The erosion of EPK and Armoricaine Kaolin in the ESTD reveals they have similar physicochemical characteristics. When prepared through consolidation, the critical shear stress of both Kaolin materials is less than 10 Pa. In erosion tests, the shear stress deceases with the erosion when the soil position keeps unchanged. The mass loss after intermittent running can be used to calculate the erosion rate of tested soil specimens.

VI REFERENCES

Briaud, J. L., Ting, F. C. K., Chen, H. C., Cao, Y., Han, S. W., and Kwak, K. W. (2001). ‘‘Erosion function apparatus for scour rate predictions.’’ *J. Geotech. Geoenviron. Eng.*, 127 (2): 105–113.

Chevalier, C. and Haghighi, I. (2011). *The Progress report on TFHRC-IFSTTAR collaboration in highway infrastructure*. French Institute of Sciences and Technology for Transport, Development and Networks (IFSTTAR), Paris, France.

Dunn, I. S. (1959). Tractive resistance of cohesive soils. *Journal of Soil Mechanics and Foundation Division*, 85 (SM3): 1 – 24.

Guo, J. (2007). Buffer law and transitional roughness effect in turbulent open-channel flows. *Proceedings of IAHR 5th International Symposium on Environmental Hydraulics (ISEH V), Boyer, D. and Alexandrova, O. Ed.*, Tempe, Arizona.

Hanson, G. J. (1991). Development of a jet index to characterize erosion resistance of soils in earthen spillways. *Trans. ASAE,* 34(5): 2015–2020.

Hanson, G. J., and Cook, K. R. (2004). Apparatus, test procedures and analytical methods to measure soil erodibility in situ. *Applied Engineering in Agriculture*, 20(4): 455-462.

Lim, S. S. (2006). *Experimental investigation of erosion in variably saturated clay soils*. Ph. D. dissertation, The University of New South Wales, Sydney, Australia.

McNiel J., Taylor C., and Lick W. (1996). Measurement of erosion of undisturbed bottom sediments with depth. *J. Hydraul. Engr.*, 122(6): 316-324.

Moore W. L. and Masch F. D. (1961). Experiment on the scour resistance of cohesive sediments. *Presentation before the Symposium on Sedimentation,* American Geophysical Union, Washington D. C.

Partheniades, E. (2009). *Cohesive sediments in open channels: properties, transport and applications*. Elsevier.

Raudkivi, A. J., and Tan, S. K. (1984). Erosion of cohesive sediments. *Journal of Hydraulic Research*, 22(4): 217-233.

Shan, H. (2010). *Experimental study on incipient motion of non-cohesive and cohesive sediments*. Ph. D. dissertation, University of Nebraska-Lincoln, Lincoln, NE.

Shan, H., Wagner, A., Kerenyi, K., and Guo, J. (2011). Velocity distribution in a channel for erosion research in cohesive soils. *Proceedings of the 34th IAHR congress*, Brisbane, Australia.

Sheppard, D. M., and Bloomquist, D. (2005). *Water erosion of Florida rock materials*. FDOT BC354 RPWO #12, Tallahassee, Florida.

Trammell, M. A. (2004). *Laboratory apparatus and methodology for determining water erosion rates of erodible rock and cohesive sediments*. MS thesis, The University of Florida, Gainesville, FL.

Wan, C.F., and Fell, R. (2004). Investigation of rate of erosion of soils in embankment dams. *J. Geotech. Geoenviron. Eng.*, 130(4), 373-380.